Spectral functions via numerical analytic continuation

Ralf-Arno Tripolt

EMMI Workshop - Functional Methods in Strongly Correlated Systems

Hirschegg, Kleinwalsertal, Austria, March 31 - April 6, 2019

Outline

Schlessinger Point Method (SPM)

- definition and simple examples

Analytic continuation of Euclidean data

- test case: spectral function and analytic structure of the Breit-Wigner propagator
- FRG, DSE and lattice data: spectral function and analytic structure of the gluon and ghost propagator

Summary and outlook

Schlessinger Point Method (SPM)

Given a finite set of N data points (x_i, f_i) we construct the rational interpolant $p(x)/q(x)$ with polynomials $p(x)$ and $q(x)$ that is given by the continued fraction

$$p(x)/q(x) = C_N(x) = \cfrac{f_1}{1 + \cfrac{a_1(x-x_1)}{1 + \cfrac{a_2(x-x_2)}{\vdots\, a_{N-1}(x-x_{N-1})}}},$$

where the coefficients a_i are given recursively by $a_1 = \frac{f_1/f_2 - 1}{x_2 - x_1}$ and

$$a_i = \frac{1}{x_i - x_{i+1}} \left(1 + \frac{a_{i-1}(x_{i+1} - x_{i-1})}{1+} \frac{a_{i-2}(x_{i+1} - x_{i-2})}{1+} \cdots \frac{a_1(x_{i+1} - x_1)}{1 - f_1/f_{i+1}} \right)$$

The polynomials $(p(x), q(x))$ are of order $(N/2 - 1, N/2)$ for an even number of input points and $((N-1)/2, (N-1)/2)$ for an odd number of input points

[L. Schlessinger, Physical Review, Volume 167, Number 5 (1968)]
[R.W. Haymaker and L. Schlesinger, Mathematics in Science and Engineering, Volume 71, Chapter 11 (1970)]
[H.J. Vidberg and J.W. Serene, Journal of Low Temperature Physics, Vol. 29, Nos. 3/4 (1977)]
[R.-A. T., I. Haritan, J. Wambach, N. Moiseyev, Physics Letters B 774 (2017) 411-416]
[R.-A. T., P. Gubler, M. Ulybyshev, L. v. Smekal, Comput.Phys.Commun. 237 (2019) 129-142]

Analytic Continuation and Radius of Convergence

- an analytic continuation into the complex plane can be performed by choosing x in $C_N(x)$ to be complex, i.e. $x = \alpha e^{i\theta}$
- rational interpolants can exactly reproduce polar singularities, thus extending the 'radius of convergence' to the first non-polar singularity, e.g. a branch point
- even a branch cut may be well approximated by a series of poles of the rational fraction
- a rational fraction can have only one sheet in the complex plane - a many-sheeted function can only be reconstructed on a single sheet

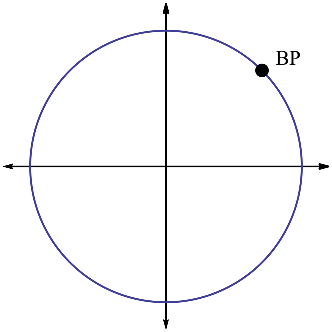

[R. de Montessus de Ballore, Bull. Soc. Math. France 30, 28 (1902)]
[P. Masjuan, J.J. Sanz-Cillero, Eur.Phys.J. C73 (2013) 2594]

Simple Example: $f(x) = 1/(x + 100)$

- we use 2 input points for the SPM
- can we reconstruct the function?

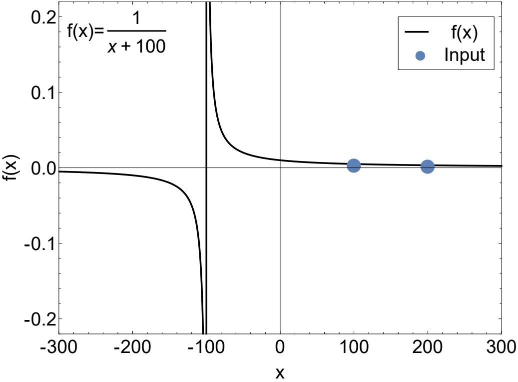

Simple Example: $f(x) = 1/(x + 100)$

- Only 2 input points are needed to reconstruct $f(x) = \frac{1}{x+100}$
- it is the "first guess" of the method

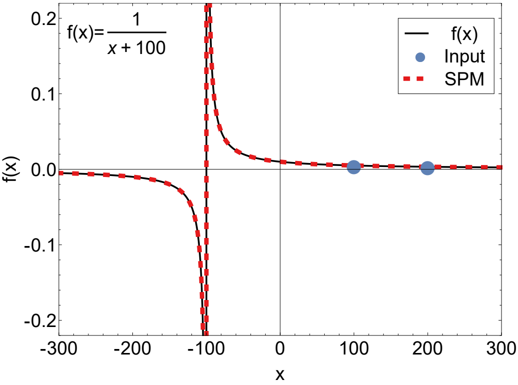

Another simple example: $f(x) = x$

- we use 3 input points for the SPM
- can we reconstruct the function?

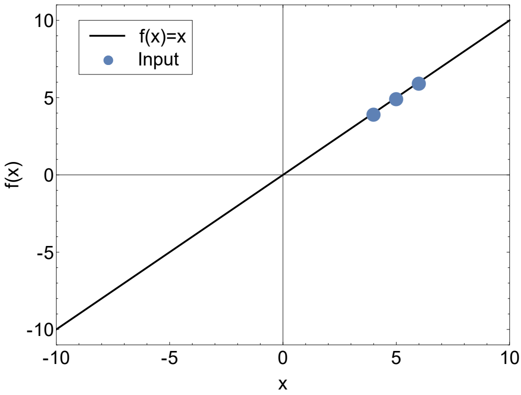

Another simple example: $f(x) = x$

- 3 input points are needed to reconstruct $f(x) = x$
- with 15 digits precision one obtains for example

$$f(x) = \frac{22 + 1.8 \cdot 10^{15} x}{1.8 \cdot 10^{15} - x} \approx x$$

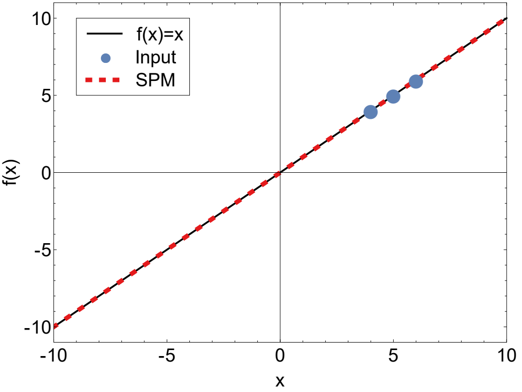

Another example: $f(x) = e^x$

- we use 11 input points
- can we reconstruct the function?

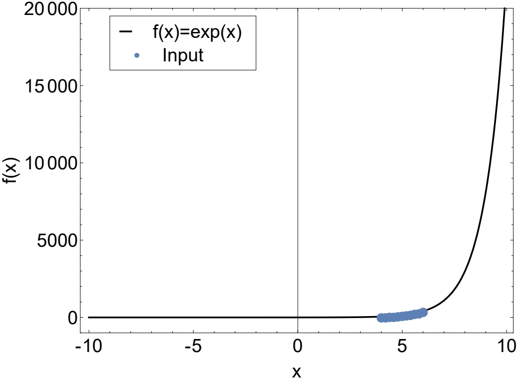

Another example: $f(x) = e^x$

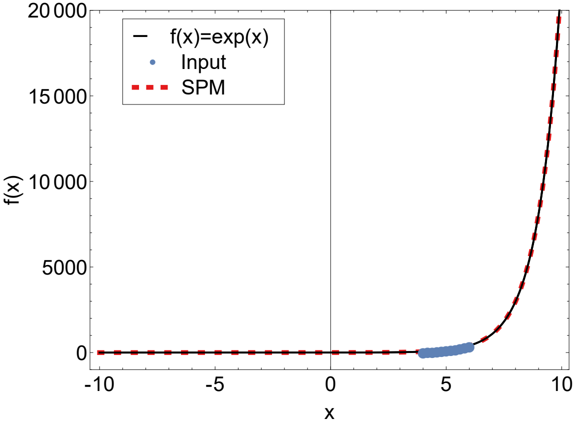

- for 11 input points we obtain

$$f(x) = \frac{263504 + 170536\,x + 46451\,x^2 + 10389\,x^3 + 756\,x^4 + 148\,x^5}{265568 - 98809\,x + 15473\,x^2 - 1274\,x^3 + 55\,x^4 - x^5}$$

Another example: $f(x) = e^x$

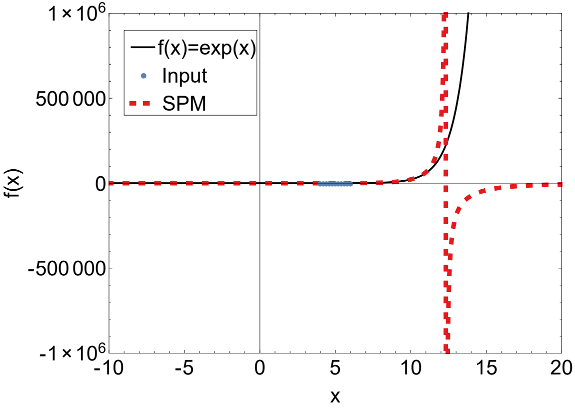

- for 11 input points we obtain

$$C_N(x) = \frac{263504 + 170536\,x + 46451\,x^2 + 10389\,x^3 + 756\,x^4 + 148\,x^5}{265568 - 98809\,x + 15473\,x^2 - 1274\,x^3 + 55\,x^4 - x^5}$$

What is a spectral function?

$$\rho(\omega) = 2\,\mathsf{Im}D(p_0 \to -i(\omega + i0^+))$$

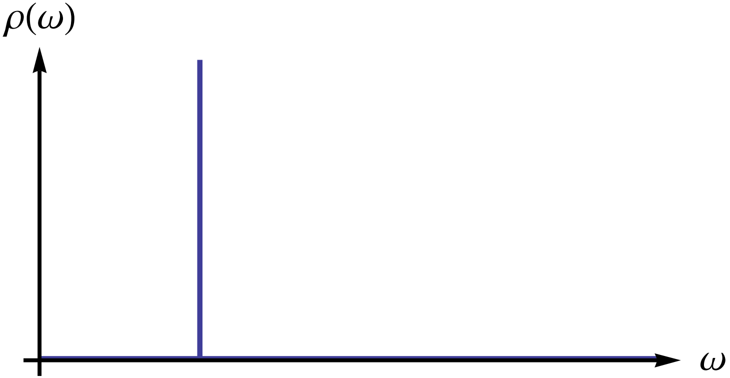

What is a spectral function?

$$\rho(\omega) = 2\,\mathrm{Im}D(p_0 \to -i(\omega + i0^+))$$

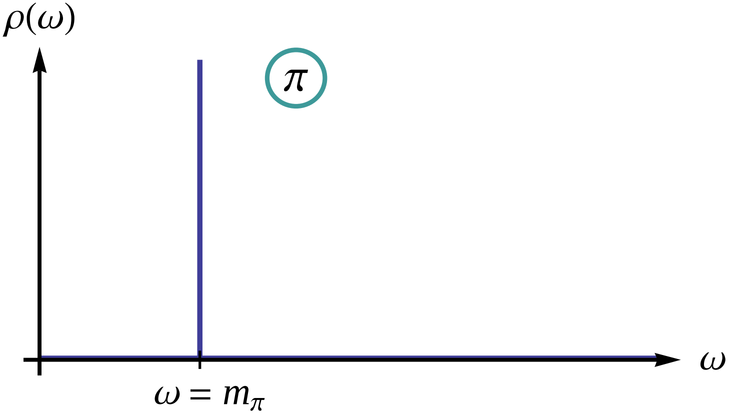

What is a spectral function?

$$\rho(\omega) = 2\,\mathrm{Im}D(p_0 \to -i(\omega + i0^+))$$

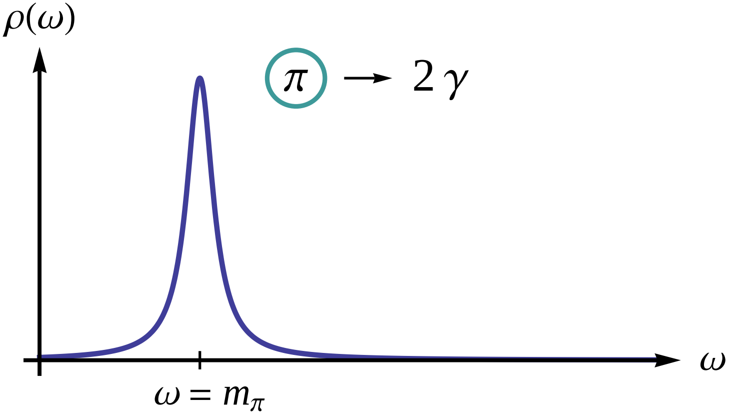

What is a spectral function?

$$\rho(\omega) = 2\,\mathrm{Im} D(p_0 \to -i(\omega + i0^+))$$

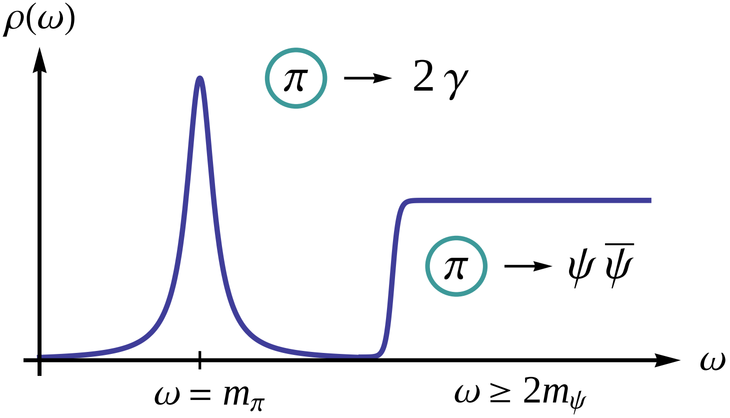

Källén-Lehmann spectral representation

$$\rho(\omega) = 2\,\mathrm{Im}D(p_0 \to -i(\omega + i0^+))$$

$$D(p_0) = \frac{1}{2\pi}\int_{-\infty}^{\infty} \frac{2\omega\rho(\omega)}{\omega^2 + p_0^2} d\omega$$

The spectral function thus allows access to many observables, e.g. transport coefficients like the shear viscosity:

- $$\eta = \frac{1}{24}\lim_{\omega\to 0}\lim_{|\vec{p}|\to 0}\frac{1}{\omega}\int d^4x\ e^{ipx}\left\langle\left[T_{ij}(x), T^{ij}(0)\right]\right\rangle$$

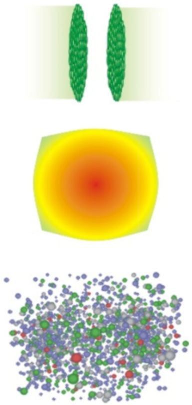

[B. Mueller, arXiv: 1309.7616]

The analytic continuation problem

Calculations at finite temperature are often performed using imaginary energies:

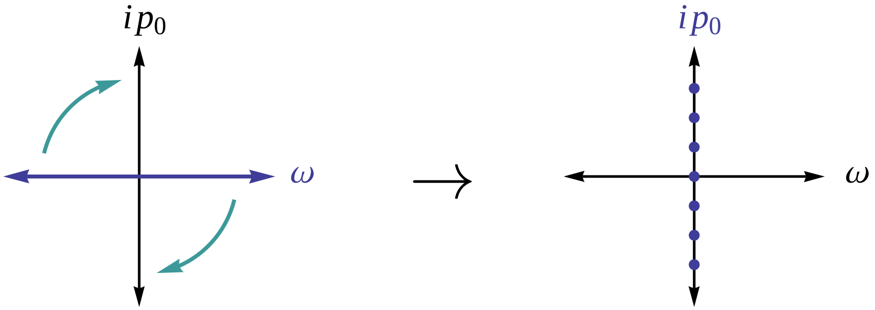

The analytic continuation problem

Analytic continuation problem: How to get back to real energies?

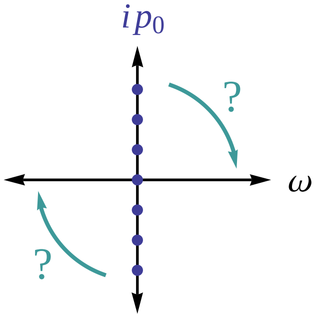

Breit-Wigner (BW) propagator

$$D(p_0) = \frac{1}{2\pi} \frac{1}{(p_0 + \Gamma)^2 + M^2}$$

$$\rho(\omega) = 2\,\mathrm{Im} D(p_0 \to -i(\omega + i0^+))$$
$$= \frac{1}{\pi} \frac{2\Gamma\omega}{(\omega^2 - \Gamma^2 - M^2)^2 + 4\Gamma^2\omega^2}$$

$$D(p_0) = \frac{1}{2\pi} \int_{-\infty}^{\infty} \frac{2\omega\rho(\omega)}{\omega^2 + p_0^2} d\omega$$

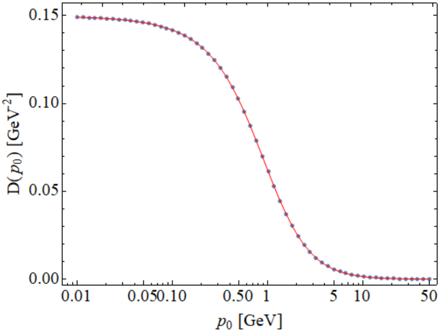

We will use $M = 4\Gamma = 1$ GeV and
60 input points for the SPM.

BW propagator in the complex p_0 plane

The poles are perfectly reconstructed with the SPM:

exact:

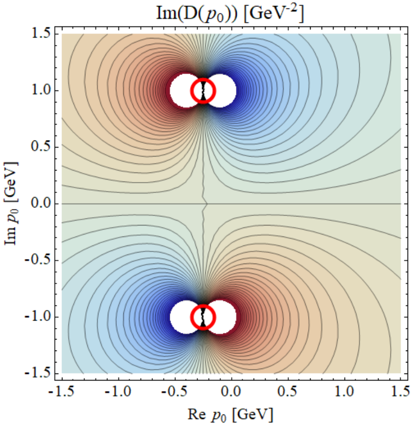

reconstructed:

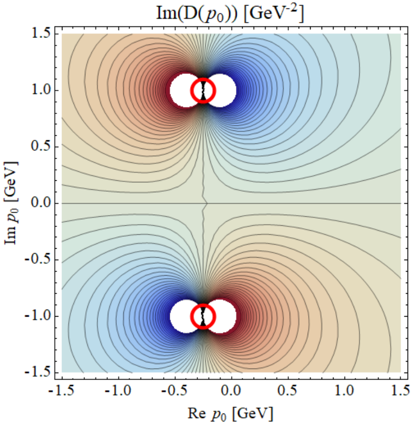

BW propagator in the complex p_0 plane

For $N = 60$ input points the reconstructed propagator has 30 poles and 29 zeroes. Unphysical poles are (nearly) canceled by the zeroes: they have small residues.

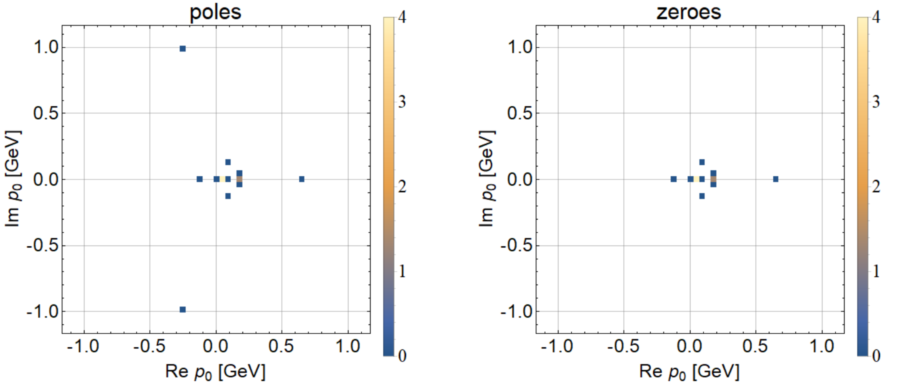

BW propagator in the complex p_0 plane

The physical poles can be identified by using a threshold for the residues:

exact:

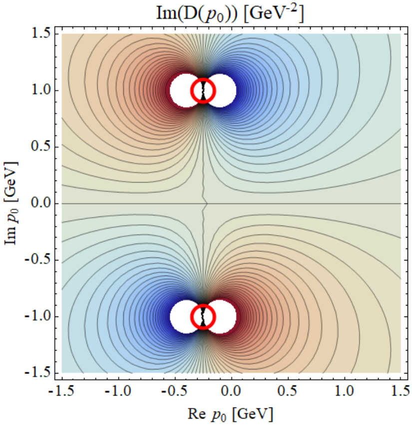

reconstructed poles:

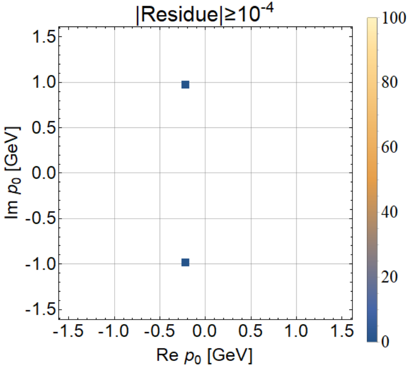

BW propagator in the complex p_0^2 plane

The branch cut is reconstructed as a series of poles:

exact:

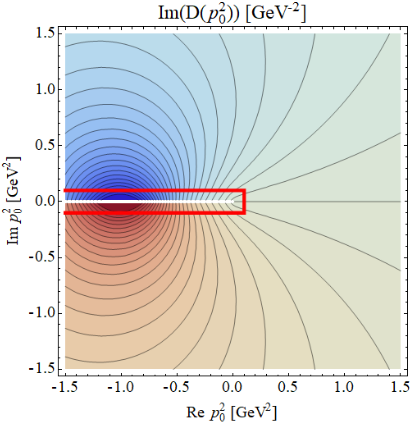

reconstructed:

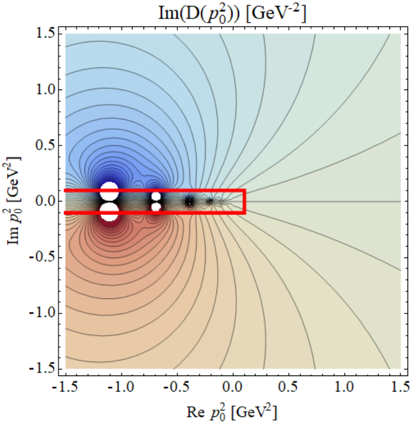

BW propagator in the complex p_0^2 plane

The branch cut is more clearly visible in a histogram, showing the location of the poles for 100 random subsets of the 60 input points.

exact:

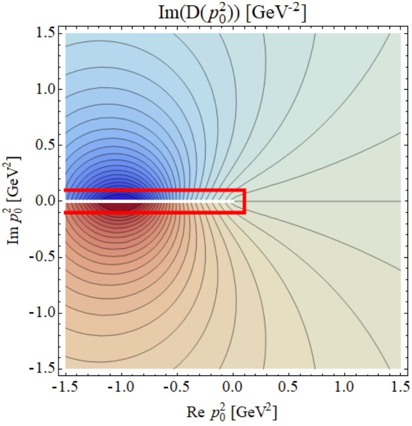

reconstructed poles:

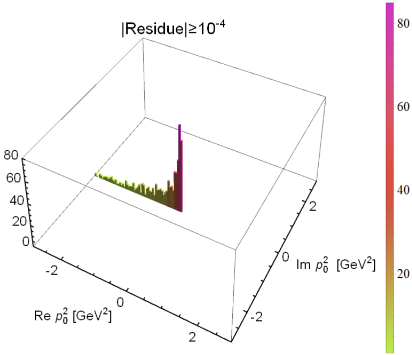

BW spectral function

The spectral functions is obtained as $\rho(\omega) = 2\,\mathrm{Im}D(p_0 \to -i(\omega + i0^+))$

and fulfills $D(p_0) = \frac{1}{2\pi}\int_{-\infty}^{\infty} \frac{2\omega\rho(\omega)}{\omega^2+p_0^2} d\omega$.

reconstructed spectral function:

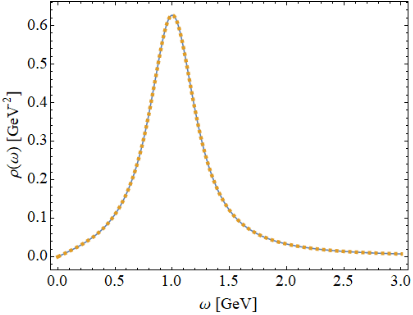

reconstructed propagator:

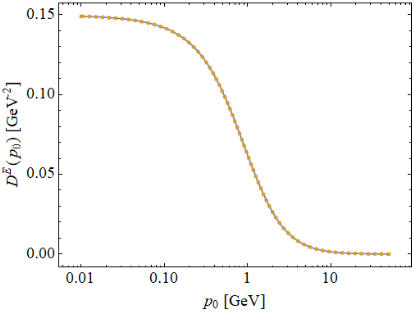

BW propagator with complex poles

$$D(p_0) = \frac{1}{2\pi}\frac{1}{(p_0+\Gamma)^2+M^2} + \sum_{j=1}^{n}\frac{Z_j}{p_0^2 - z_j}$$

$$\rho(\omega) = 2\,\mathrm{Im}D(p_0 \to -i(\omega + i0^+))$$
$$= \frac{1}{\pi}\frac{2\Gamma\omega}{(\omega^2-\Gamma^2-M^2)^2+4\Gamma^2\omega^2}$$

$$D(p_0) = \frac{1}{2\pi}\int_{-\infty}^{\infty}\frac{2\omega\rho(\omega)}{\omega^2+p_0^2}d\omega + \sum_{j=1}^{n}\frac{Z_j}{p_0^2 - z_j}$$

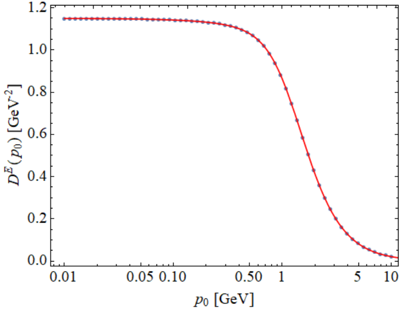

We will use $M = 4\Gamma = 1$ GeV, $Z_1 = Z_2 = 1$, $z_{1,2} = (-1 \pm i)$ GeV^2.

[D. Binosi and R.-A. T., in preparation]

[Y. Hayashi, K.-I. Kondo, arXiv: 1812.03116]

[F. Siringo, EPJ Web Conf. 137, 13017 (2017)]

BW with complex poles in the p_0 plane

The poles are perfectly reconstructed with the SPM:

exact:

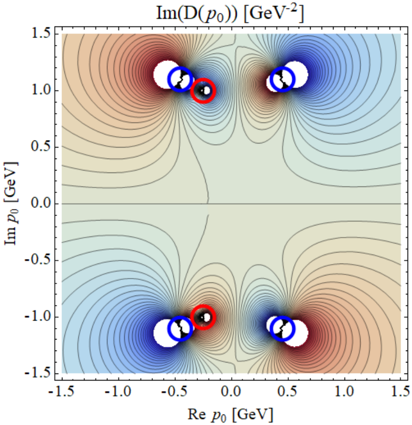

reconstructed:

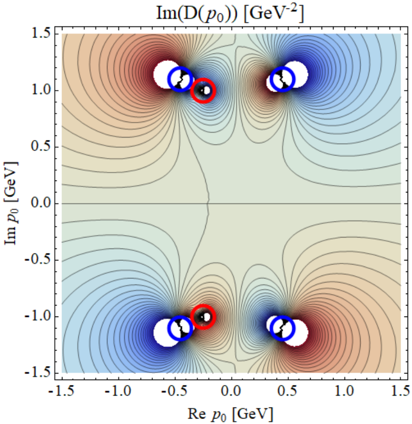

BW with complex poles in the p_0^2 plane

The branch cut is reconstructed as a series of poles:

exact:

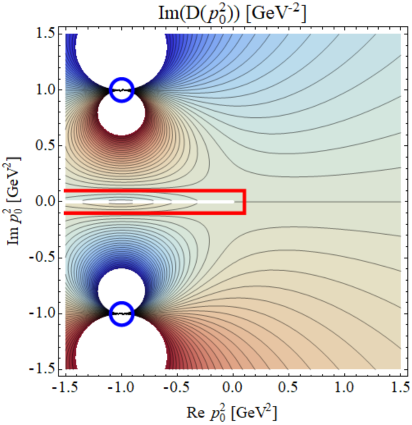

reconstructed:

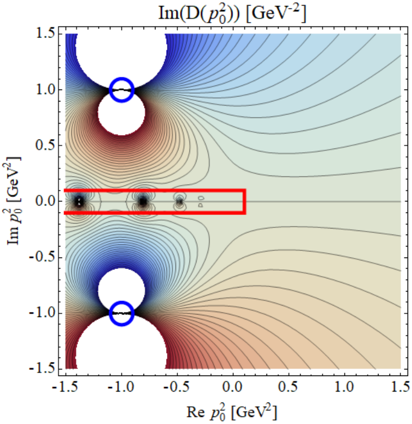

BW with complex poles in the p_0^2 plane

Both the branch cut and the poles are visible in the histogram:

exact:

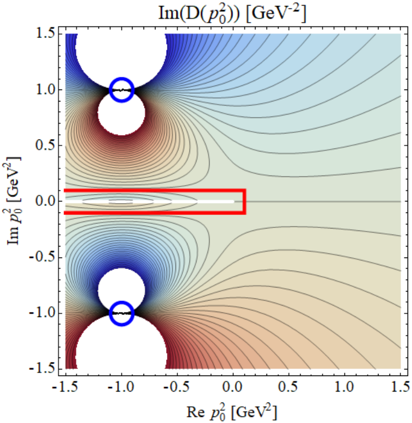

reconstructed poles:

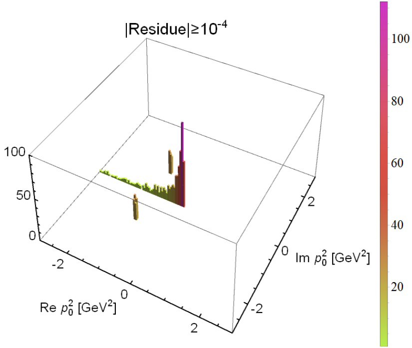

BW propagator with complex poles

The spectral functions is obtained as $\rho(\omega) = 2\,\mathrm{Im}D(p_0 \to -i(\omega + i0^+))$

and fulfills the generalized spectral representation.

reconstructed spectral function:

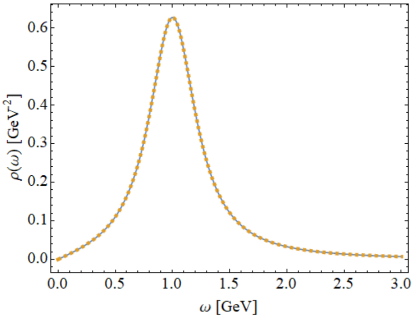

reconstructed propagator:

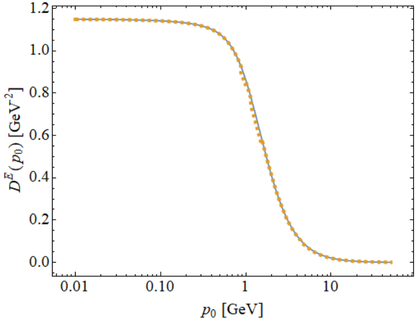

BW propagator with noise

$$D(p_0) = \frac{1}{2\pi} \frac{1}{(p_0 + \Gamma)^2 + M^2}$$

$$\rho(\omega) = 2\,\mathrm{Im} D(p_0 \to -i(\omega + i0^+))$$
$$= \frac{1}{\pi} \frac{2\Gamma\omega}{(\omega^2 - \Gamma^2 - M^2)^2 + 4\Gamma^2\omega^2}$$

$$D(p_0^2) = \frac{1}{2\pi} \int_{-\infty}^{\infty} \frac{2\omega\rho(\omega)}{\omega^2 + p_0^2} d\omega$$

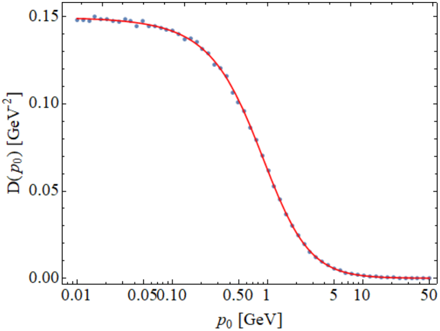

We will use $M = 4\Gamma = 1$ GeV and add noise: $y_i \to y_i(1 + \varepsilon r_i)$ with $\varepsilon = 10^{-2}$ and r_i a random number drawn from a normal distribution with zero mean and unit standard deviation.

BW propagator with noise in the p_0 plane

The poles are still very well reconstructed with the SPM:

exact:

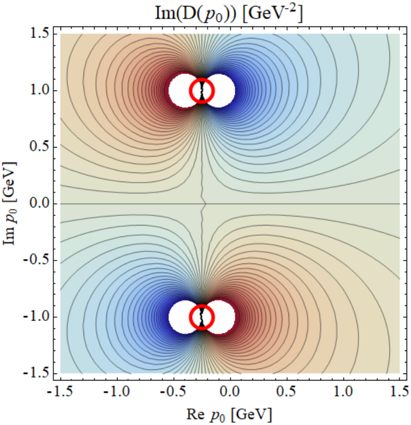

reconstructed:

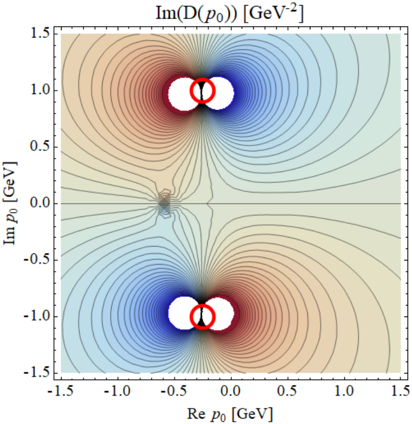

BW propagator with noise in the p_0^2 plane

The branch cut is reconstructed as a series of poles:

exact:

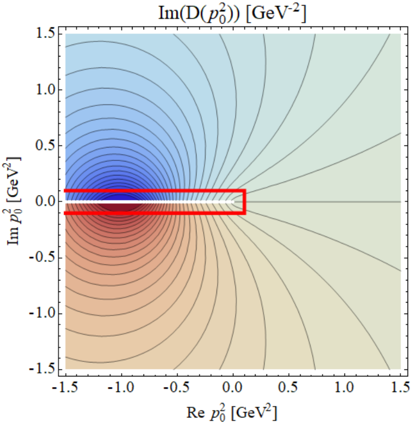

reconstructed:

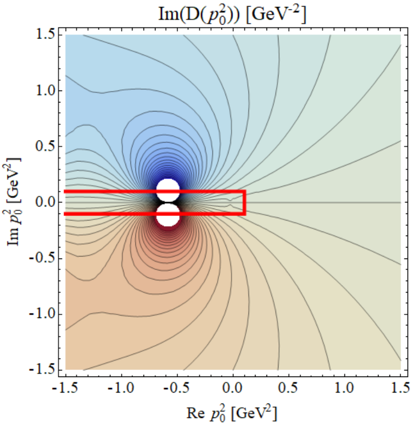

BW propagator with noise in the p_0^2 plane

The branch cut is reconstructed as a series of poles:

exact:

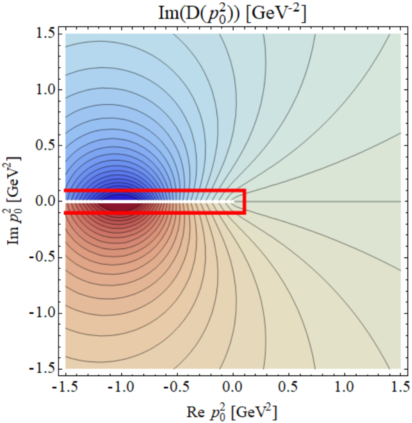

reconstructed:

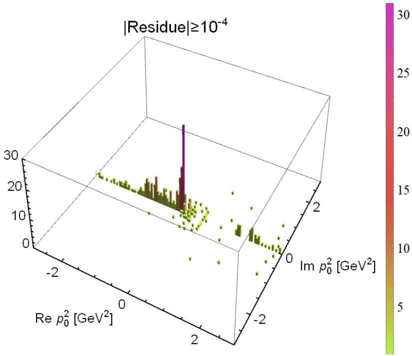

BW propagator with noise

The spectral functions is obtained as $\rho(\omega) = 2\,\mathrm{Im}D(p_0 \to -i(\omega + i0^+))$

and fulfills $D(p_0) = \frac{1}{2\pi}\int_{-\infty}^{\infty} \frac{2\omega\rho(\omega)}{\omega^2+p_0^2}d\omega$.

reconstructed spectral function:

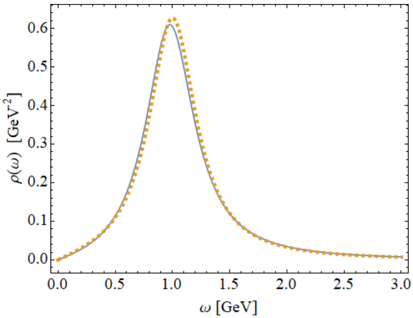

reconstructed propagator:

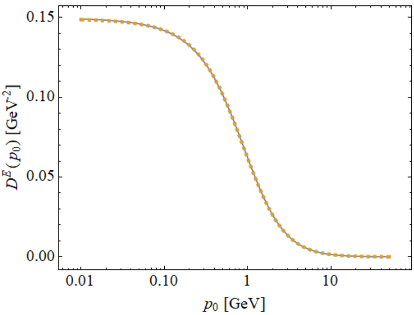

BW with complex poles and noise

$$D(p_0) = \frac{1}{2\pi}\frac{1}{(p_0+\Gamma)^2+M^2} + \sum_{j=1}^{n}\frac{Z_j}{p_0^2 - z_j}$$

$$\rho(\omega) = 2\,\mathrm{Im}D(p_0 \to -i(\omega + i0^+))$$
$$= \frac{1}{\pi}\frac{2\Gamma\omega}{(\omega^2-\Gamma^2-M^2)^2+4\Gamma^2\omega^2}$$

$$D(p_0^2) = \frac{1}{2\pi}\int_{-\infty}^{\infty}\frac{2\omega\rho(\omega)}{\omega^2+p_0^2}d\omega + \sum_{j=1}^{n}\frac{Z_j}{p_0^2 - z_j}$$

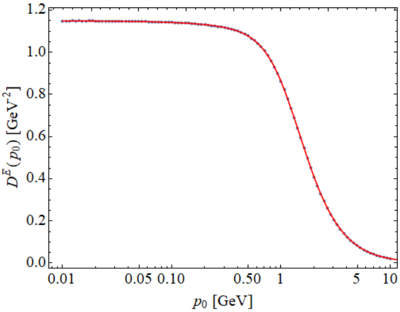

We will use $M = 4\Gamma = 1$ GeV, $Z_1 = Z_2 = 1$, $z_{1,2} = (-1 \pm i)$ GeV^2. and add noise: $y_i \to y_i(1 + \varepsilon r_i)$ with $\varepsilon = 10^{-3}$ and r_i a random number drawn from a normal distribution with zero mean and unit standard deviation.

BW with complex poles and noise in the p_0 plane

Some poles are not found when using a single input data set only:

exact:

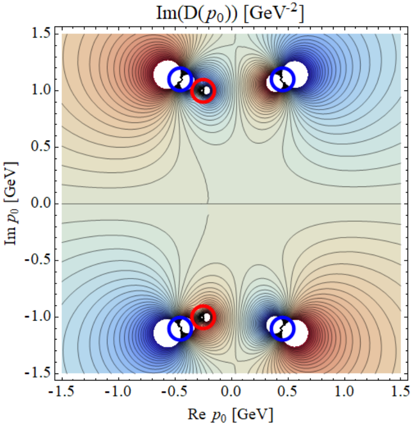

reconstructed:

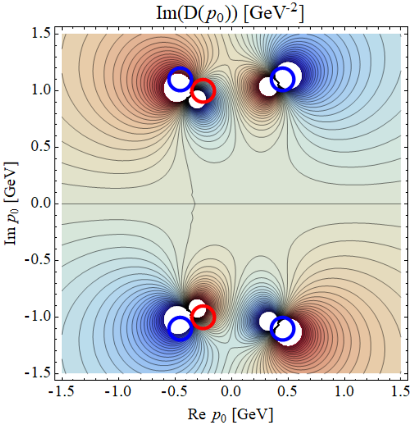

BW with complex poles and noise in the p_0^2 plane

The poles are correctly reconstructed:

exact:

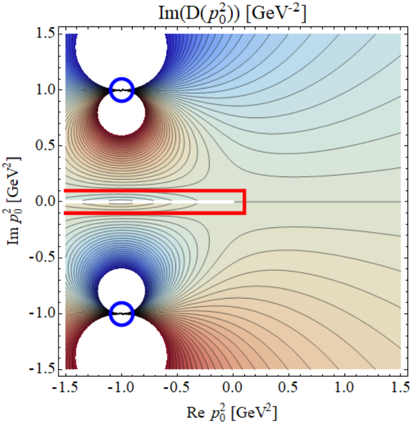

reconstructed:

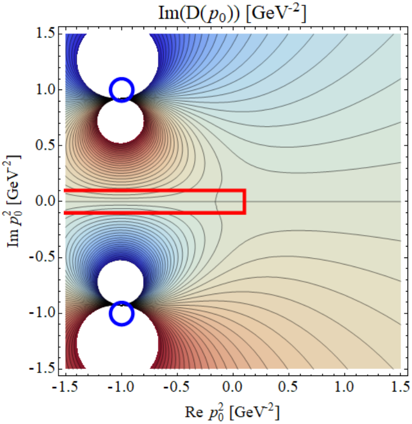

BW with complex poles and noise in the p_0^2 plane

The poles and the branch cut are clearly visible in the histogram:

exact:

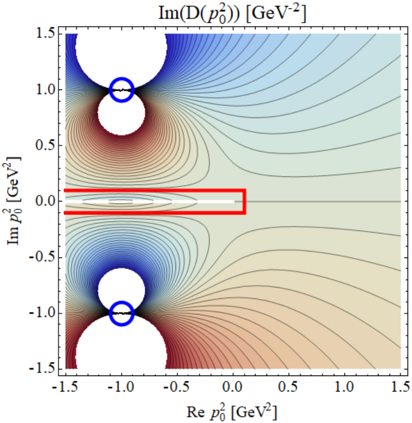

reconstructed:

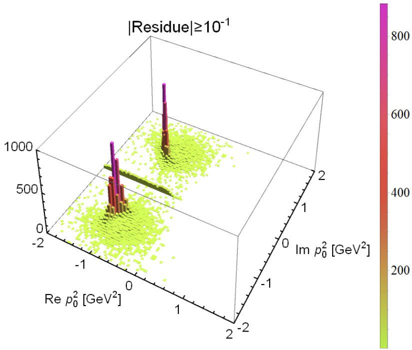

BW with complex poles and noise

The spectral functions is obtained as $\rho(\omega) = 2\,\mathrm{Im}D(p_0 \to -i(\omega + i0^+))$

and fulfills the generalized spectral representation.

reconstructed spectral function:

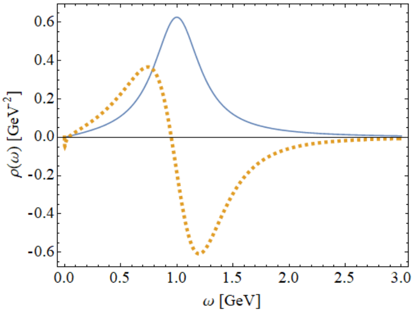

reconstructed propagator:

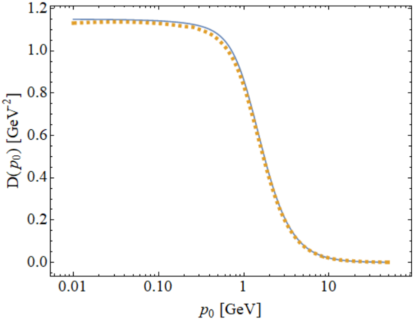

Improved SPM algorithm

1. Select $N = 50$ points randomly from the set of $M > N$ points (x_i, y_i) for $D(p_0)$

2. Apply the SPM to this subset of points and construct $C_N(x)$

3. Obtain the spectral function as $\rho(\omega) = 2\text{Im}C_N(-i(\omega + i0^+))$

4. Identify the relevant complex poles and compute $D_{\text{rec}}(p_0)$

5. Calculate the χ^2-deviation of the reconstr. propagator, $X^2 = \sum_{i=1}^{M} \frac{(D_{\text{rec}}(x_i) - D(x_i))^2}{D(x_i)}$

6. repeat 1.-5. $L = 5000$ times and identify the input point (x_j, y_j) that appears most often among the $K = 200$ best subsets, i.e. those with the smallest X^2

7. repeat 1.-6. but always use the points (x_j, y_j) among the $N = 50$ points until all optimal input points have been identified

[D. Binosi and R.-A. T., in preparation]

BW with complex poles and noise

We apply the improved SPM algorithm to the BW propagator with complex poles:

[D. Binosi and R.-A. T., in preparation]

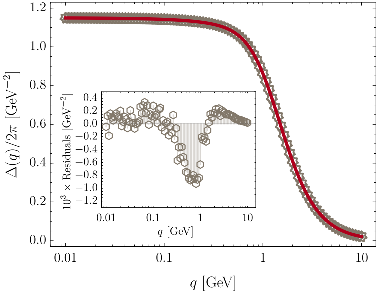

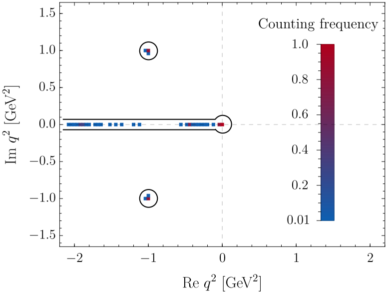

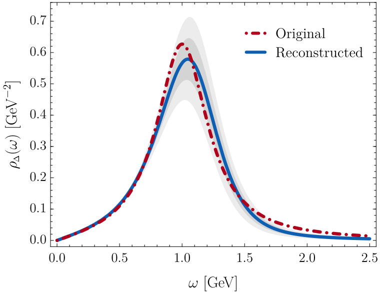

FRG data on the gluon propagator

We will study FRG data on the gluon in Landau gauge SU(3) Yang-Mills theory:

Data set 1: Fit (with noise $\epsilon = 10^{-6}$) from Cyrol et al., SciPost Phys. 5, 065 (2018)

Data set 2: Same as 1 but with additional complex conjugate poles in p_0^2

Data set 3: FRG data from Cyrol et al., Phys. Rev. D 94, 054005 (2016)

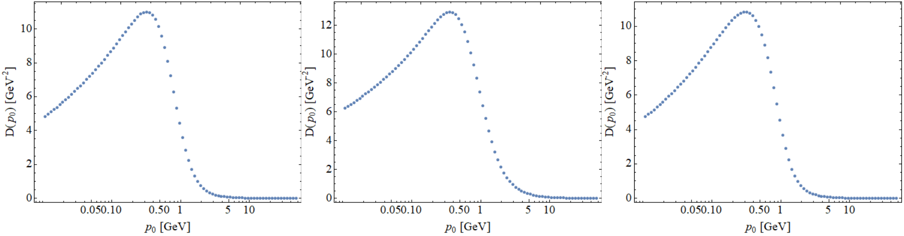

Data set 1

$$\hat{G}^{\text{pole}}_{\text{Ans}}(p_0) = \sum_{k=1}^{N_{\text{ps}}} \prod_{j=1}^{N^{(k)}_{\text{pp}}} \left(\frac{\hat{\mathcal{N}}_k}{(\hat{p}_0 + \hat{\Gamma}_{k,j})^2 + \hat{M}^2_{k,j}} \right)^{\delta_{k,j}} , \quad \hat{G}^{\text{poly}}_{\text{Ans}}(p_0) = \sum_{j=1}^{N_{\text{poly}}} \hat{a}_k \left(\hat{p}_0^2\right)^{\frac{j}{2}}$$

$$\hat{G}^{\text{asy}}_{\text{Ans}}(p_0) = (\hat{p}_0^2)^{-1-2\alpha} \left[\log\left(1 + \frac{\hat{p}_0^2}{\hat{\lambda}^2}\right)\right]^{-1-\beta} , \quad G_{\text{Ans}}(p_0) = \mathcal{K} \hat{G}^{\text{pole}}_{\text{Ans}}(p_0) \hat{G}^{\text{poly}}_{\text{Ans}}(p_0) \hat{G}^{\text{asy}}_{\text{Ans}}(p_0)$$

$\hat{\mathcal{N}}_1$ 1.33678	α -0.428714	β -0.777213	$\hat{\lambda}$ 1.75049		
$\hat{a}_1$ 0.454024	$\hat{a}_2$ 0.241017	$\hat{a}_3$ 3.10257	$\hat{a}_4$ -1.30804	$\hat{a}_5$ 0.63701	
$\hat{\Gamma}_{1,1}$ 0.100169	$\hat{\Gamma}_{1,2}$ 0.100141	$\hat{\Gamma}_{1,3}$ 2.36445	$\hat{\Gamma}_{1,4}$ 1.5564	$\hat{\Gamma}_{1,5}$ 1.22013	$\hat{\Gamma}_{1,6}$ 1.15102
$\hat{M}_{1,1}$ 0.849883	$\hat{M}_{1,2}$ 0.849902	$\hat{M}_{1,3}$ 2.52171	$\hat{M}_{1,4}$ 2.44035	$\hat{M}_{1,5}$ 3.6016	$\hat{M}_{1,6}$ 2.36723
$\delta_{1,1}$ 1.61116	$\delta_{1,2}$ 1.94095	$\delta_{1,3}$ -2.54586	$\delta_{1,4}$ 1.89765	$\delta_{1,5}$ 0.168592	$\delta_{1,6}$ 0.296215

[A. K. Cyrol, J. M. Pawlowski, A. Rothkopf, N. Wink, SciPost Phys. 5, 065 (2018)]

Data set 2

$$\hat{G}^{\text{pole}}_{\text{Ans}}(p_0) = \sum_{k=1}^{N_{\text{ps}}} \prod_{j=1}^{N^{(k)}_{\text{pp}}} \left(\frac{\hat{\mathcal{N}}_k}{(\hat{p}_0 + \hat{\Gamma}_{k,j})^2 + \hat{M}^2_{k,j}} \right)^{\delta_{k,j}} , \quad \hat{G}^{\text{poly}}_{\text{Ans}}(p_0) = \sum_{j=1}^{N_{\text{poly}}} \hat{a}_k \left(\hat{p}_0^2\right)^{\frac{j}{2}}$$

$$\hat{G}^{\text{asy}}_{\text{Ans}}(p_0) = (\hat{p}_0^2)^{-1-2\alpha} \left[\log\left(1 + \frac{\hat{p}_0^2}{\hat{\lambda}^2}\right) \right]^{-1-\beta}$$

$$G_{\text{Ans}}(p_0) = \mathcal{K} \hat{G}^{\text{pole}}_{\text{Ans}}(p_0) \hat{G}^{\text{poly}}_{\text{Ans}}(p_0) \hat{G}^{\text{asy}}_{\text{Ans}}(p_0) + \frac{3}{p_0^2 - (-0.25 + i)} + \frac{3}{p_0^2 - (-0.25 - i)}$$

$\hat{\mathcal{N}}_1$ 1.33678	α -0.428714	β -0.777213	$\hat{\lambda}$ 1.75049		
$\hat{a}_1$ 0.454024	$\hat{a}_2$ 0.241017	$\hat{a}_3$ 3.10257	$\hat{a}_4$ -1.30804	$\hat{a}_5$ 0.63701	
$\hat{\Gamma}_{1,1}$ 0.100169	$\hat{\Gamma}_{1,2}$ 0.100141	$\hat{\Gamma}_{1,3}$ 2.36445	$\hat{\Gamma}_{1,4}$ 1.5564	$\hat{\Gamma}_{1,5}$ 1.22013	$\hat{\Gamma}_{1,6}$ 1.15102
$\hat{M}_{1,1}$ 0.849883	$\hat{M}_{1,2}$ 0.849902	$\hat{M}_{1,3}$ 2.52171	$\hat{M}_{1,4}$ 2.44035	$\hat{M}_{1,5}$ 3.6016	$\hat{M}_{1,6}$ 2.36723
$\delta_{1,1}$ 1.61116	$\delta_{1,2}$ 1.94095	$\delta_{1,3}$ -2.54586	$\delta_{1,4}$ 1.89765	$\delta_{1,5}$ 0.168592	$\delta_{1,6}$ 0.296215

[A. K. Cyrol, J. M. Pawlowski, A. Rothkopf, N. Wink, SciPost Phys. 5, 065 (2018)]

Data set 3

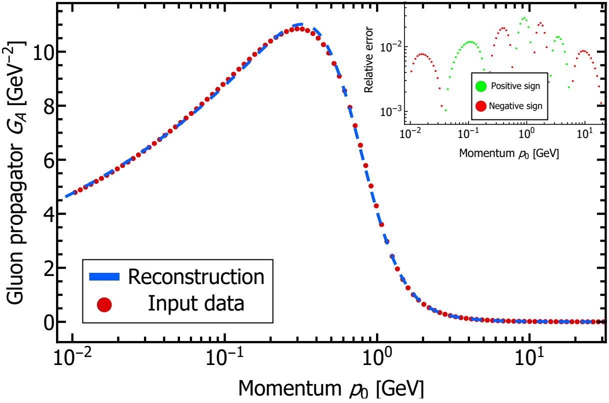

[A. K. Cyrol, L. Fister, M. Mitter, J. M. Pawlowski, N. Strodthoff, Phys. Rev. D 94, 054005 (2016)]

[A. K. Cyrol, J. M. Pawlowski, A. Rothkopf, N. Wink, SciPost Phys. 5, 065 (2018)]

FRG data on the gluon propagator

Data set 1:

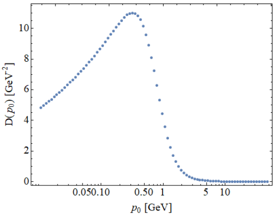

Data set 2:

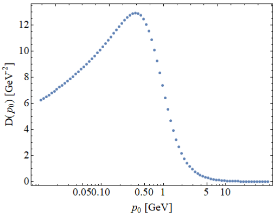

Data set 3:

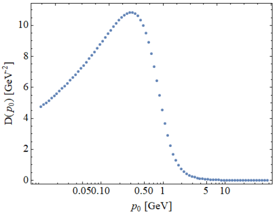

exact:

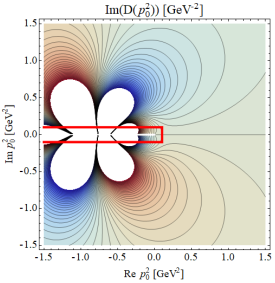

exact:

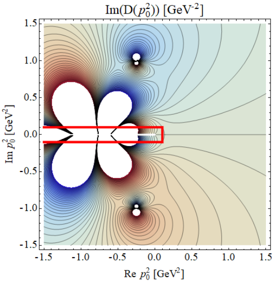

exact:

?

FRG data on the gluon propagator

Data set 1, exact:

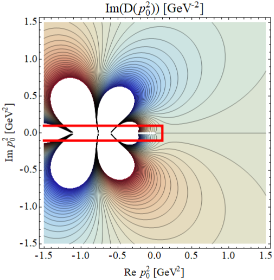

Data set 2, exact:

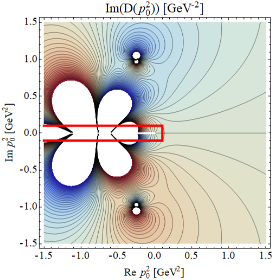

Data set 3, exact:

?

reconstructed:

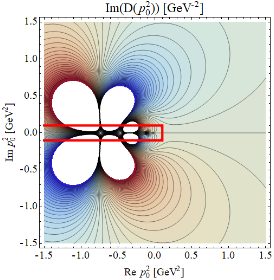

reconstructed:

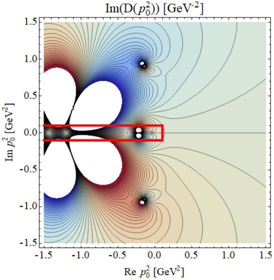

reconstructed:

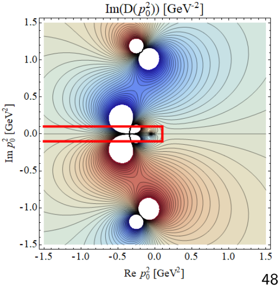

FRG data on the gluon propagator

Data set 1, exact:

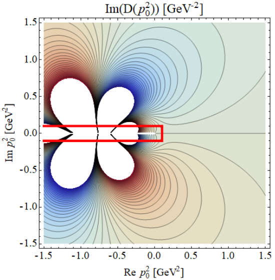

Data set 2, exact:

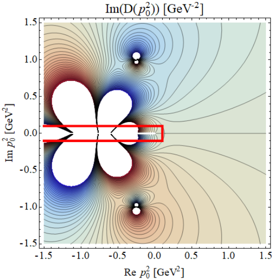

Data set 3, exact:

?

reconstructed:

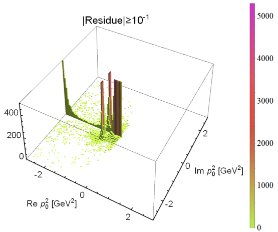

reconstructed:

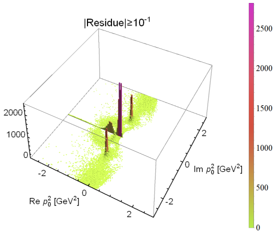

reconstructed:

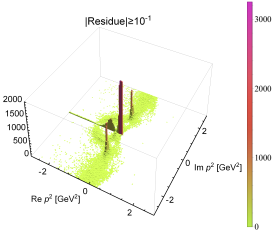

FRG data on the gluon propagator

We apply the improved SPM algorithm to the data from Cyrol et al., Phys. Rev. D 94, 054005 (2016).

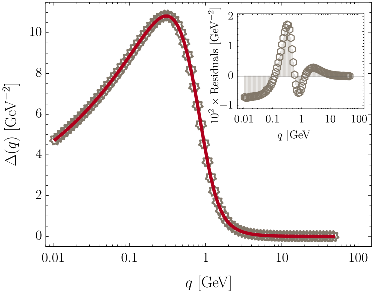

The data show evidence for complex conjugate poles.

The reconstructed spectral function has the correct IR and UV behavior:

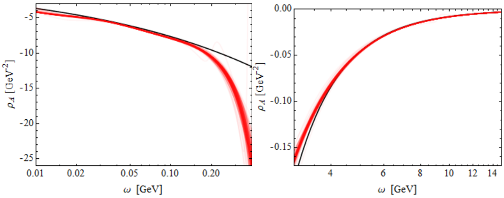

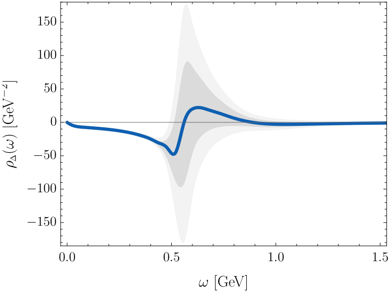

[D. Binosi and R.-A. T., in preparation]

FRG data on the gluon propagator

We apply the improved SPM algorithm to the data from Cyrol et al., Phys. Rev. D 94, 054005 (2016).

The data show evidence for complex conjugate poles.

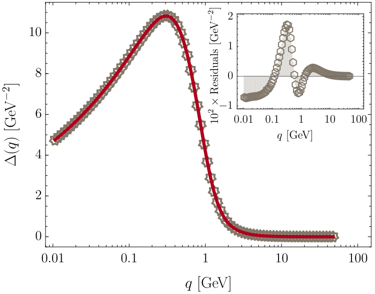

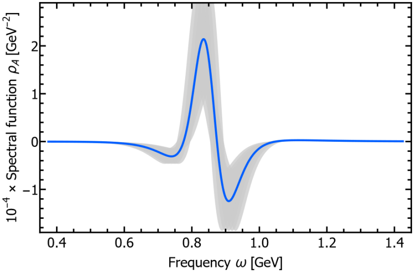

[Cyrol et al., Phys. Rev. D 94, 054005 (2016)]

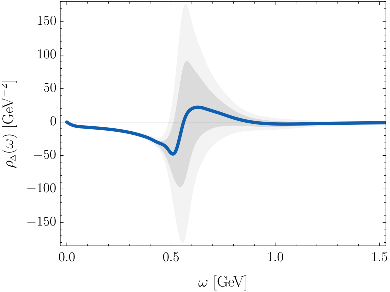

[D. Binosi and R.-A. T., in preparation]

DSE data on the gluon propagator

We apply the improved SPM algorithm to data from Strauss, Fischer, Kellermann, PRL 109, 252001 (2012).

The data show evidence for complex conjugate poles.

[D. Binosi and R.-A. T., in preparation]

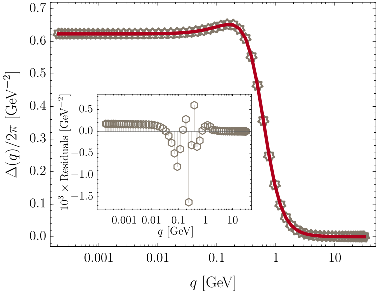

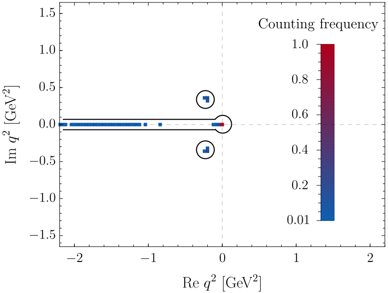

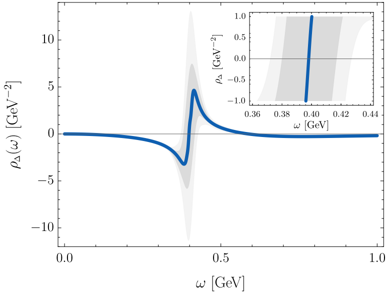

DSE data on the gluon propagator

We apply the improved SPM algorithm to data from Strauss, Fischer, Kellermann, PRL 109, 252001 (2012).

The data show evidence for complex conjugate poles.

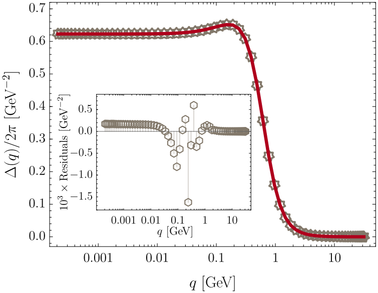

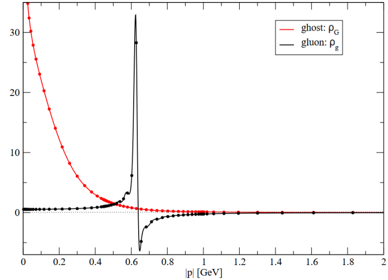

[Strauss et al., PRL 109, 252001 (2012)]

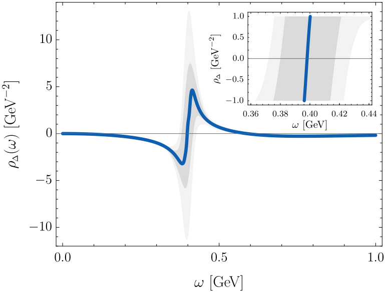

[D. Binosi and R.-A. T., in preparation]

Lattice data on the gluon propagator

We apply the improved SPM algorithm to data obtained on a 64^4 lattice with $\beta = 6.0$ in SU(3) Yang-Mills theory, Duarte, Oliveira, Silva, Phys. Rev. D 94, 014502 (2016).

The data show evidence for complex conjugate poles.

[D. Binosi and R.-A. T., in preparation]

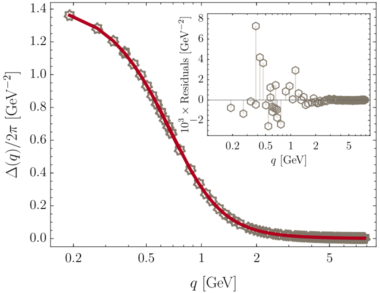

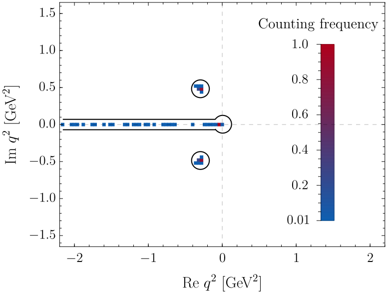

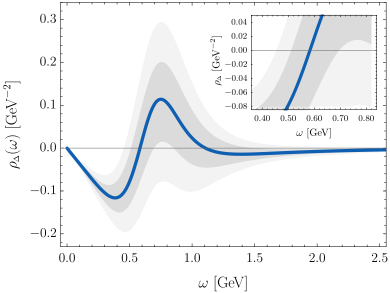

Lattice data on the gluon propagator

We apply the improved SPM algorithm to data obtained on a 64^4 lattice with $\beta = 6.0$ in SU(3) Yang-Mills theory from Duarte, Oliveira, Silva, Phys. Rev. D 94, 014502 (2016).

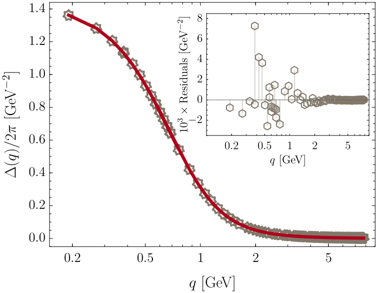

Tikhonov reconstruction:

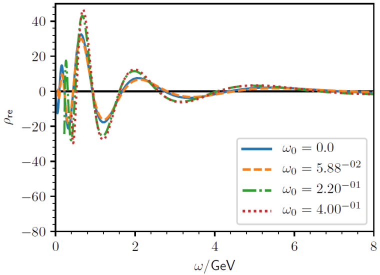

[Dudal, Oliveira, Roelfs, Silva, arXiv:1901.05348]

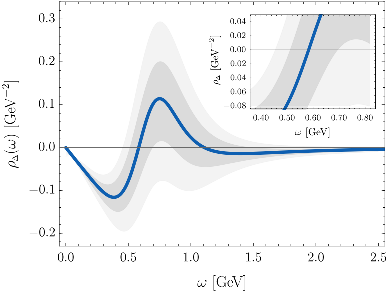

[D. Binosi and R.-A. T., in preparation]

DSE data on the ghost propagator

We apply the improved SPM algorithm to data from Strauss, Fischer, Kellermann, PRL 109, 252001 (2012).

The ghost propagator only exhibits a branch cut.

[D. Binosi and R.-A. T., in preparation]

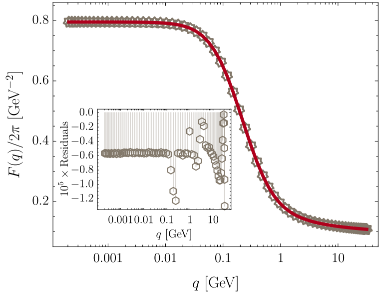

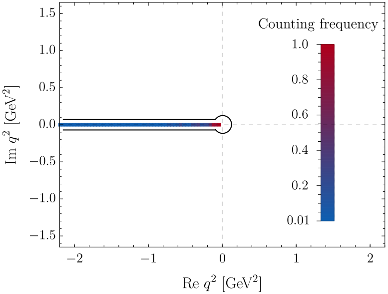

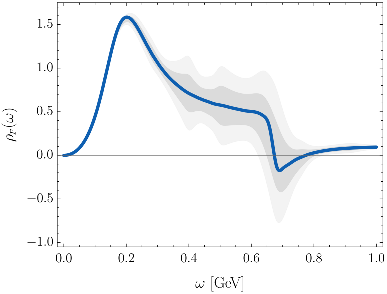

DSE data on the ghost propagator

We apply the improved SPM algorithm to data from Strauss, Fischer, Kellermann, PRL 109, 252001 (2012).

The ghost propagator only exhibits a branch cut.

[D. Binosi and R.-A. T., in preparation]

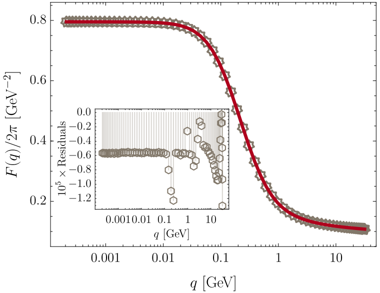

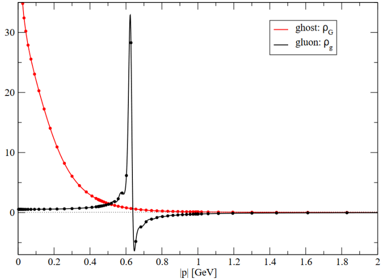

[Strauss et al., PRL 109, 252001 (2012)]

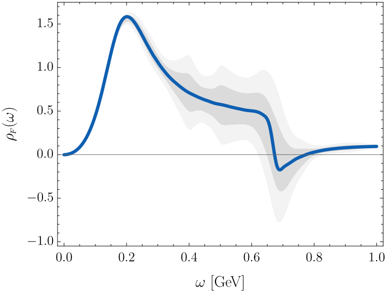

[D. Binosi and R.-A. T., in preparation]

Lattice data on the ghost propagator

We apply the improved SPM algorithm to data obtained on a 64^4 lattice with $\beta = 6.0$ in SU(3) Yang-Mills theory, Duarte, Oliveira, Silva, Phys. Rev. D 94, 014502 (2016).

The ghost propagator only exhibits a branch cut.

[D. Binosi and R.-A. T., in preparation]

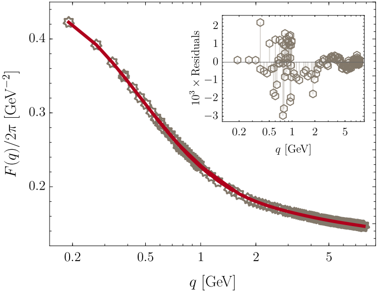

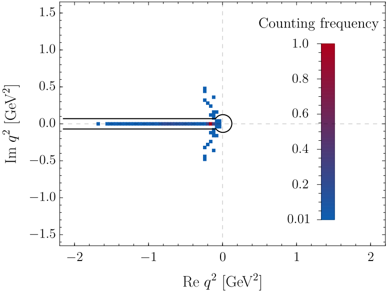

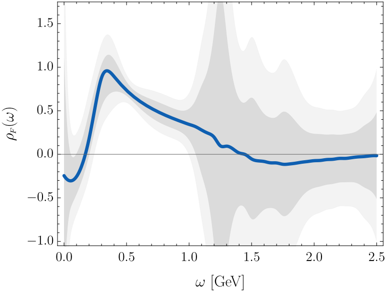

Lattice data on the ghost propagator

We apply the improved SPM algorithm to data obtained on a 64^4 lattice with $\beta = 6.0$ in SU(3) Yang-Mills theory, Duarte, Oliveira, Silva, Phys. Rev. D 94, 014502 (2016).

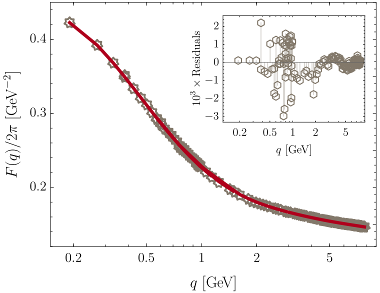

The ghost propagator only exhibits a branch cut.

Tikhonov reconstruction:

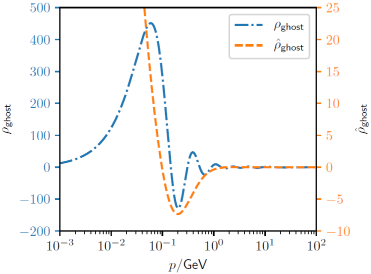

[Dudal, Oliveira, Roelfs, Silva, arXiv:1901.05348]

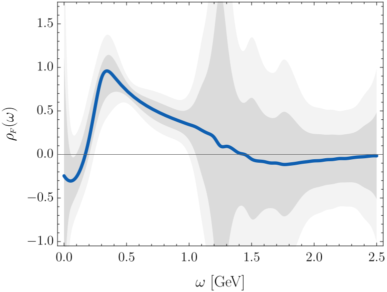

[D. Binosi and R.-A. T., in preparation]

Summary

We applied the Schlessinger point method (SPM) to FRG, DSE and lattice data on the Landau gauge SU(3) Yang-Mills gluon and ghost propagator in order to determine their analytic structure in the complex q^2 plane and to reconstruct the corresponding spectral functions:

- the gluon and ghost propagators show a branch cut at $q^2 \leq 0$
- in addition, we find evidence for complex conjugate poles in the gluon propagator